Communication in Mathematical Modeling and Applications

http://ntmsci.com/cmma

Finite element method for a fluid flow in a non-uniform channel

Tesfahun Berhane, Mebratu F. Wakeni

Department of Mathematics, Bahir Dar University, Ethiopia
Department of Mathematics and Applied Mathematics, University of Cape Town, South Africa

Received: 9 November 2016, Accepted: 17 December 2016
Published online: 21 December 2016.

Abstract: A numerical method based on the finite element method is used for an investigation of viscous, incompressible fluid flowing in a channel with slowly varying cross-section with absorbing walls. The proposed mathematical model can be applied to understand the flow behaviour of a fluid in renal tubules. The method is not restricted by the parameters in the problem such as wave number, permeability parameter, amplitude ratio and Reynolds number. The effects of these parameters on the transverse velocity and mean pressure drop is studied and the results are presented graphically. Results show that the parameters cause a significant change on the flow.

Keywords: Fluid flow, Finite element method, Non-uniform channel.

1 Introduction

One of the excretory organ of the human body is kidney. Kidneys excrete most of the end products of body metabolism and they control concentrations of most of the constituents of body fluids. The basic functional unit of kidney is nephron. Each kidney contains over a million tiny units (of nephrons), all similar in structure and function. Each nephron functions independently and in most instances it is sufficient to study the function of nephron to understand the mechanism of kidney in terms of mathematical models.

In nephrons, the portion after the Bowman's capsule is called proximal convoluted tubule, which is narrower than rest of the tube and non-uniform in nature. It is the place where most of useful substances, like water, glucose and electrolytes are reabsorbed back into the plasma and unwanted substances pass into urine. Thus it is of interest to study the flow in proximal tubule using mathematical models.

Study of viscous fluid flow in channels of varying cross section with permeable wall is significant because of its application to both physiological and engineering flow problems. The flow of fluid in a renal tubule has been studied by different authors. Macey [1] formulated the problem as the flow of an incompressible viscous fluid through a circular tube with linear rate of reabsorption at the wall. Whereas, Kelman [2] found that the bulk flow in the proximal tubule decays exponentially with the axial distance. Then, Macey [3] used this condition to solve the equations of motion and mentioned that the longitudinal velocity profile is parabolic and the drop in mean pressure is proportional to the mean axial flow. Marshall and Trowbridge [4] and Palatt et.al [5] used physical conditions existing at the rigid permeable tube instead of prescribing the flux at the wall as a function of axial distance.

The representation of a proximal tubule as a uniform tube with constant wall permeability is obviously an idealization. Radhakrishnamacharya et al [6] considered a non-uniform geometry to model renal tubule while the previous studies

* Corresponding author e-mail: tesfahunb2002@gmail.com

considered it uniform. They made an attempt to understand the flow through the renal tubule by studying the hydrodynamical aspects of an incompressible viscous fluid in a circular tube of varying cross-section with reabsorption at the wall. Following similar approach, Chandra and Prasad [7] analyzed fluid flow in rigid tube of slowly varying cross-section by considering different geometries. Also they investigated the problem by considering fluid exchange across the permeable wall governed by Starling's hypothesis. Chaturani and Ranganatha [8] studied fluid flow through a diverging/converging tube with variable wall permeability. They obtained approximate analytical solution for the case that the flux at the wall depends on wall permeability and transboundary pressure drop. Recently, Muthu and Tesfahun [9] have studied the fluid flow in nonuniform rigid wavy channel of varying cross section and presented the effects of slope parameter, reabsorption coefficient on the transverse velocity and mean pressure drop.

In all the above studies, the method used to solve the governing equations of the fluid motion is perturbation method of solution by taking small nonuniform tube parameter/curvature parameter. In this paper, the Navier-Stokes equations governing the flow of an incompressible viscous fluid through a wavy non-uniform permeable channel are solved numerically by using the finite element method. The effects of wave number (δ), reabsorption coefficient (α), amplitude ratio (ε) and Reynolds number on the transverse velocity, stream function and mean pressure drop are studied without restrictions on the parameters of the problem, in principle.

The boundary of the channel walls are assumed to be symmetric about x axis and vary with x. It is taken as

$$\eta(x) = d + k_1 x + a \sin(\frac{2\pi x}{\lambda}) \tag{1}$$

where d is the half width of the channel at the inlet (at $x = 0$). k_1 is a constant whose magnitude depends on the length of the channel exit and inlet dimensions, a is the amplitude and λ is the wave length (see Fig.1). Here, we assume $k_1 \ll 1$ to model the slowly varying slope.

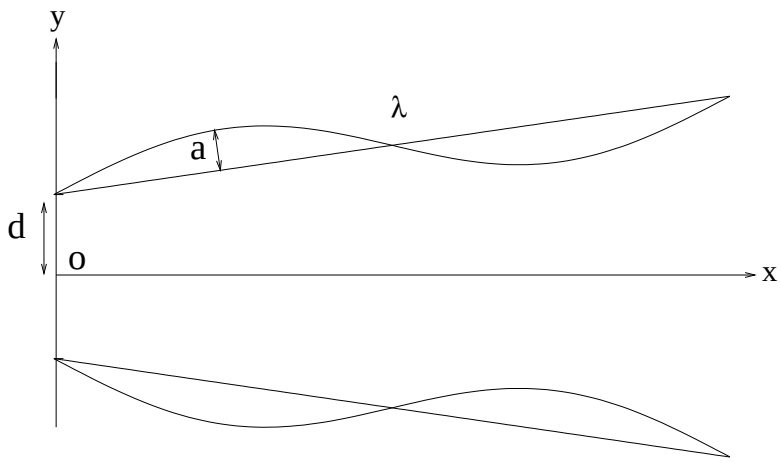

Fig. 1: Geometry of the problem.

2 Mathematical formulation

In this section we summarize the equation governing the flow of a fluid flowing through channel. Two types of formulation are discussed, namely the *velocity-pressure* and *vorticity-stream function*. The boundary conditions relevant to the problem are also presented consistently in both the two formulations.

2.1 Velocity-pressure formulation

Consider an incompressible fluid flowing through a radially symmetric channel with cross-section varying slowly along the axis as given by equation 1. The motion of the fluid is assumed to be laminar, steady and symmetric. As a result we consider a section of the channel in 2D with domain denoted by Ω. The channel is long enough to neglect the initial and end effects. The equations governing the motion of such fluid formulated in terms of the primitive fields (velocity-pressure formulation) are given by, (see for example [10])

$$\begin{aligned} \nabla \cdot \boldsymbol{u} &= 0 \\ (\boldsymbol{u} \cdot \nabla)\boldsymbol{u} &= -\nabla P + \nu \nabla^2 \boldsymbol{u}, \end{aligned} \tag{2}$$

where $\boldsymbol{u} = ui + vj$ the velocity vector field, P the pressure, ν the kinematic viscosity parameter. The symbols $\nabla = (\partial/\partial x)i + (\partial/\partial y)j$ and $\nabla^2 = \nabla \cdot \nabla$ are the gradient and Laplacian differential operators on Ω, respectively. The first equation of (2) is the continuity accounting for the incompressibility condition. The equations of motion (2) are subjected to the following boundary conditions

(a) **The tangential velocity at the wall is zero**. The tangent vector to the boundary at x is $\boldsymbol{T} = i + \frac{\mathrm{d}}{\mathrm{d}x}\eta(x)j$. Then

$$0 = \boldsymbol{T} \cdot \boldsymbol{u} = u + \frac{\mathrm{d}}{\mathrm{d}x}\eta(x)v \qquad \text{on the upper wall with } y = \eta(x). \tag{3}$$

(b) **Inlet/Outlet boundaries**: Based on our assumption we consider a symmetrical inlet boundary condition. That is,

$$u(0,y) = f(y). \tag{4}$$

where f is some function which is symmetrical with respect to the x-axis with $f(d) = 1$, and the outlet boundary condition:

$$u = g(y), \tag{5}$$

where g is symmetric with respect to the x-axis.

(c) The **re-absorption** has been accounted for by considering the bulk flow as a decreasing function of x along the wall. That is, the flux across a cross-section is given as

$$Q(x) = \int_0^{\eta(x)} v(x,y)dy = Q_0 F(\alpha x), \tag{6}$$

where $F(\alpha x) = 1$ when $\alpha = 0$ and decreases with x, the constant $\alpha \geq 0$ is the re-absorption coefficient, and Q_0 is the flux across the cross-section at $x = 0$.

In 2D the Navier-Storckes equations (2) composed of three partial differential equations with three variables (two velocity components and one pressure field). There have been some simpler formulations developed, among this the most common is the *vorticity-stream function* ($\psi - \omega$) formulation. In this formulation, the incompressibility constraint $(2)_1$ is satisfied apriori from the construction itself. As a result the pressure does not appear in the formulation as unknown. Rather, it can be obtained from the primary unknown fields as a post-process.

2.2 The vorticity-stream function formulation

The stream function ψ and the vorticity ω are scalar valued fields defined on Ω, defined by

$$u = \frac{\partial \psi}{\partial y}, \qquad v = -\frac{\partial \psi}{\partial x}, \qquad \text{and} \qquad \omega = \frac{\partial v}{\partial x} - \frac{\partial u}{\partial y}. \tag{7}$$

To non-dimensionalized the formulation we use the following scaling

$$x' = \frac{x}{\lambda}, \qquad y' = \frac{y}{d}, \qquad \eta' = \frac{\eta}{d},$$
$$\psi' = \frac{\psi}{Q_0}, \qquad \alpha' = \alpha\lambda, \qquad p' = \frac{d^2}{\mu Q_0}p,$$

where x', y', η', ψ', α', and p' are the dimensionless counterparts of x, y, η, ψ, α, and p respectively. The vorticity-stream function ($\psi-\omega$) formulation of the governing equations (2) in the dimensionless form are given by (after dropping the primes)

$$\begin{aligned} \boldsymbol{A}\nabla^2\omega &= \delta R_e \nabla\omega\cdot(\boldsymbol{B}\nabla\psi) \\ \boldsymbol{A}\nabla^2\psi &= -\omega, \end{aligned} \tag{8}$$

where $\delta = d/\lambda$ is a constant resulting from differentiation with respect to the non-dimensional spatial variables x and y, $R_e = Q_0/\nu$ is the Reynolds number, $\boldsymbol{A}$ is symmetric and $\boldsymbol{B}$ is anti-symmetric second-order tensors given by

$$\boldsymbol{A} = \begin{bmatrix} \delta^2 & 0 \\ 0 & 1 \end{bmatrix}, \qquad \boldsymbol{B} = \begin{bmatrix} 0 & 1 \\ -1 & 0 \end{bmatrix} \tag{9}$$

The non-dimensional form of the boundary boundary conditions, discussed above, in terms of the $\psi-\omega$ are:

(a) The tangential component of the velocity vector equates to the normal derivative of the stream function at the boundary; that is, we recall that the tangent vector to the top section of the wall is given by $\boldsymbol{T} = i + \frac{\mathrm{d}}{\mathrm{d}x}\eta(x)$, hence the outward normal on the boundary is $\boldsymbol{n} = -\frac{\mathrm{d}}{\mathrm{d}x}\eta(x)i + j$ so that $\boldsymbol{T}\cdot\boldsymbol{n} = 0$. To this end, the boundary condition (3) is translated to free Neumann-type condition of the form

$$0 = \frac{\partial\psi}{\partial n} = \boldsymbol{n}\cdot\nabla\psi = \boldsymbol{T}\cdot\boldsymbol{u}. \tag{10}$$

Similarly the same boundary condition is prescribed at the opposite side of the boundary with $y = -\eta(x)$.

(b) The stream function ψ is also prescribed at the inlet/outlet boundaries so that the x-component of the velocity field is parabola and conformable with the adjacent boundary conditions (ψ is continuous everywhere). That is,

$$\psi = \tilde{f}(y), \qquad \text{on the inlet boundary,} \tag{11}$$
$$\psi = \tilde{g}(y), \qquad \text{on the outlet boundary,} \tag{12}$$

where $\tilde{f}$ and $\tilde{g}$ are anti-derivatives of f and g respectively.

(c) The re-absorption boundary condition reads as

$$\psi = Q_0 F(\alpha x), \qquad \text{on the wall with } y = \eta(x). \tag{13}$$

Similarly ψ is prescribed, along the wall at the opposite side, a symmetric value, $-Q_0F(\alpha x)$.

In this problem, we consider exponentially decaying bulk flow, that is, in equation (13), F is taken as

$$F(\alpha x) = \exp[-\alpha x], \tag{14}$$

where α is the permeability coefficient.

3 Finite element approximation

In this section we present the finite element formulation of the vorticity-stream function form (7). We then continue to linearize the weak form upon which the Galerkin finite element approximation and its iterative matrix system are also formulated. In the present analysis, the governing equations (7) together with the boundary conditions (10)-(13) are solved in the finite region ABCD shown Figure 2. Although the boundary conditions for the infinite channel have been given, the present numerical method requires furthermore the conditions on the entrance section AB and the exit section CD because the numerical analysis is carried out for the finite region ABCD as discussed by [10, 12] and [11]. Due to this, the following conditions shall be introduced

(i) The y-component of the flow velocity vanishes at the inlet and outlet boundaries. That is, $v = -\partial\psi/\partial x = 0$.
(ii) The profile of the stream function ψ is given by the prescribed functions $\tilde{f}(y)$ and $\tilde{g}(y)$ at AB and CD respectively.
(iii) The only boundary condition with respect to the vorticity function ω is free Neumann boundary condition over the entire boundary. That is, $\partial\omega/\partial n = 0$ at each point on the boundary of Ω.

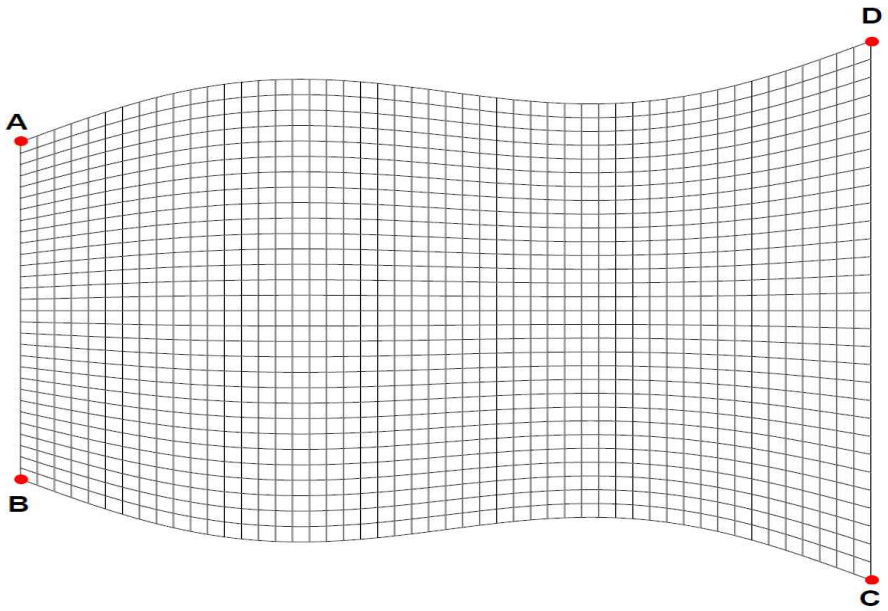

Fig. 2: Domain of the problem.

Therefore, the boundary conditions used in the analysis can be written as follows:

$$\psi = h, \qquad \text{and} \qquad \frac{\partial\psi}{\partial n} = 0, \qquad \frac{\partial\omega}{\partial n} = 0 \qquad \text{on } \Gamma = \partial\Omega, \tag{15}$$

where h is a function defined on the entire boundary Γ by

$$h = \begin{cases} \tilde{f}(y) & \text{On AB (inflow)} \\ -F(\alpha x) & \text{On BC} \\ \tilde{g}(y) & \text{On CD (outflow)} \\ F(\alpha x) & \text{On AD} \end{cases} \tag{16}$$

with $\tilde{f}(y)$ and $\tilde{g}(y)$ are functions of y, such that u is parabolic at AB and CD sections. We assume that these functions satisfy the boundary conditions so that the solution is free from discontinuities.

3.1 Variational formulation

To formulate the weak form of the problem (7) we first define the trial and weighting function spaces for both vorticity, ω, and stream function, ψ. For formal treatment of finite element procedure see, for example [14]. *Stream function trial space*

$$\mathscr{S}_\psi = \{\psi : \psi \in H^1(\Omega) \text{ and } \psi = h(x,y) \text{ on } \partial\Omega\}. \tag{17}$$

emphVorticity trial space

$$\mathscr{S}_\omega = \{\omega : \omega \in H^1(\Omega)\}. \tag{18}$$

Stream function weighting space

$$\mathscr{V}_\psi = \{\phi : \phi \in H^1(\Omega) \text{ and } \phi = 0 \text{ on } \partial\Omega\}. \tag{19}$$

Vorticity weighting space

$$\mathscr{V}_\omega = \{\varphi : \varphi \in H^1(\Omega)\}. \tag{20}$$

Since there is no Dirichelet boundary condition with respect the vorticity, ω, the vorticity trial and weighting spaces are the same, $H^1(\Omega)$. The variational problem corresponding to the system (7) together with the boundary conditions (15) reads as: Find $(\psi,\ \omega) \in \mathscr{S}_\psi \times \mathscr{S}_\omega$ such that for each $(\phi,\ \varphi) \in \mathscr{V}_\psi \times \mathscr{V}_\omega$

$$\begin{aligned} \int_\Omega \nabla\phi \cdot (\boldsymbol{A}\nabla\omega)\mathrm{d}\Omega + \delta R_e \int_\Omega \phi\nabla\omega \cdot (\boldsymbol{B}\nabla\psi)\mathrm{d}\Omega &= \int_\Gamma \phi \frac{\partial\omega}{\partial n}\mathrm{d}\Gamma \\ \int_\Omega \nabla\varphi \cdot (\boldsymbol{A}\nabla\psi)\mathrm{d}\Omega + \int_\Omega \varphi\psi\mathrm{d}\Omega &= \int_\Gamma \varphi \frac{\partial\psi}{\partial n}\mathrm{d}\Gamma. \end{aligned} \tag{21}$$

Note that, for the problem under discussion, the right hand sides of the above equations vanish as a consequence of the homogeneous Neumann boundary conditions given in equation (15).

3.2 Linearisation of the weak formulation

The weak formulation in the forms of (21) is non-linear in the unknown fields stream function ψ and vorticity ω. An iterative solution technique of Newton's type is employed to solve the non-linear problems. The method requires one to linearise the non-linear problem to generate iterative linear problems that are solved and updated sequentially until a desired level of convergence is reached (see, for example, [13] and the references therein, for detailed discussion of the concept of linearisation).

Suppose that $\mathcal{R}\ \mathcal{R} = \mathcal{R}(\psi,\ \omega)$ be a sufficiently smooth non-linear function. The linearisation of $\mathcal{R}$ is based on the first-order (Taylor's) expansion, which expressed as

$$\mathcal{R}(\psi + \delta\psi,\ \omega + \delta\omega) = \mathcal{R}(\psi,\ \omega) + \mathcal{R}'(\psi,\ \omega; \delta\psi,\ \delta\omega) + \mathcal{O}(\delta\psi,\ \delta\omega), \tag{22}$$

where $\mathcal{R}'(\psi,\ \omega; \delta\psi,\ \delta\omega)$, which we also denoted it by $D_\delta\mathcal{R}(\psi,\ \omega)$, is the directional derivative of $\mathcal{R}$ at $(\psi,\ \omega)$ in the direction of $(\delta\psi,\ \delta\omega)$ and it is defined by

$$D_\delta\mathcal{R}(\psi,\ \omega) = \mathcal{R}'(\psi,\ \omega; \delta\psi,\ \delta\omega) = \lim_{h\to 0} \frac{\mathcal{R}(\psi + h\delta\psi,\ \omega + h\delta\omega) - \mathcal{R}(\psi,\ \omega)}{h}. \tag{23}$$

To find the linearisation of the weak form (21) we take an arbitrary trial pair $(\phi,\ \varphi)$ then define $\mathcal{R}$ as a vector-valued function as

$$\mathcal{R}(\psi,\ \omega) = \begin{bmatrix} \mathcal{R}_1(\psi,\ \omega) \\ \mathcal{R}_2(\psi,\ \omega) \end{bmatrix} \tag{24}$$

where

$$\begin{aligned} \mathcal{R}_1(\psi,\ \omega) &= \int_\Omega \nabla\phi \cdot (\boldsymbol{A}\nabla\omega)\mathrm{d}\Omega + \delta R_e \int_\Omega \phi\nabla\omega \cdot (\boldsymbol{B}\nabla\psi)\mathrm{d}\Omega \\ \mathcal{R}_2(\psi,\ \omega) &= \int_\Omega \nabla\varphi \cdot (\boldsymbol{A}\nabla\psi)\mathrm{d}\Omega + \int_\Omega \varphi\psi\mathrm{d}\Omega. \end{aligned} \tag{25}$$

Hence the directional derivative $D_\delta\mathcal{R}(\psi,\ \omega)$ is computed as

$$D_\delta\mathcal{R}(\psi,\ \omega) = \begin{bmatrix} D_\delta\mathcal{R}_1(\psi,\ \omega) \\ D_\delta\mathcal{R}_2(\psi,\ \omega) \end{bmatrix} \tag{26}$$

where

$$\begin{aligned} D_\delta\mathcal{R}_1(\psi,\ \omega) &= \int_\Omega \nabla\phi \cdot (\boldsymbol{A}\nabla\ \delta\omega)\mathrm{d}\Omega + \delta R_e \int_\Omega \phi\nabla\ \delta\omega \cdot (\boldsymbol{B}\nabla\psi)\mathrm{d}\Omega + \delta R_e \int_\Omega \phi\nabla\omega \cdot (\boldsymbol{B}\nabla\ \delta\psi)\mathrm{d}\Omega \\ D_\delta\mathcal{R}_2(\psi,\ \omega) &= \int_\Omega \nabla\varphi \cdot (\boldsymbol{A}\nabla\ \delta\psi)\mathrm{d}\Omega + \int_\Omega \varphi\ \delta\psi\mathrm{d}\Omega. \end{aligned} \tag{27}$$

The Newton's scheme for the problem (21) reads as: Given that the k approximate solution $(\psi_k,\ \omega_k)$. Our objective is to find an update $(\delta\psi_k,\ \delta\omega_k)$ such that for each $(\phi,\ \varphi) \in \mathscr{V}_\psi \times \mathscr{V}_\omega$

$$D_\delta\mathcal{R}(\psi_k,\ \omega_k) = -\mathcal{R}(\psi_k,\ \omega_k). \tag{28}$$

Then the next, $k+1$, approximate solution $(\delta\psi_{k+1},\ \delta\omega_{k+1})$ is given by

$$\psi_{k+1} = \delta\psi_k + \psi_k, \quad \text{and} \quad \omega_{k+1} = \delta\omega_k + \omega_k \tag{29}$$

3.3 Galerkin approximation

Consider a triangulation $\mathcal{T}$ of $\overline{\Omega}$ into rectangular elements Ω^e, $e = 1,2,\ldots N_{el}$ such that

$$\overline{\Omega} = \bigcup_{e=1}^{N_{el}} \Omega^e. \tag{30}$$

Consider the finite element bases $\{\phi_i^h\}$ and $\{\varphi_i^h\}$ corresponding to the variations $\delta\psi$ and $\delta\omega$, respectively. The current unknown updates $\delta\psi_k$ and $\delta\omega_k$ are expressed as linear combinations of the respective basis elements:

$$\delta\psi_k = \sum_i \delta\psi^i\ \phi_i^h, \quad \text{and} \quad \delta\omega_k = \sum_i \delta\omega^i\ \varphi_i^h \tag{31}$$

where $\delta\psi^i$ and $\delta\omega^i$ are coefficient of expansion for $\delta\psi_k$ and $\delta\omega_k$ respectively.

Given the k^{th} approximate finite element solution $(\psi_k^h,\ \omega_k^h)$. Substitution of the expansions in (31) and weighting functions by the basis functions ϕ_i^h and φ_i^h into the iterative scheme (28) leads to the matrix iterative system

$$\begin{bmatrix} \mathbf{K}_k^{\psi\psi} & \mathbf{K}_k^{\psi\omega} \\ \mathbf{K}_k^{\omega\psi} & \mathbf{K}_k^{\omega\omega} \end{bmatrix} \begin{bmatrix} \boldsymbol{\delta\psi} \\ \boldsymbol{\delta\omega} \end{bmatrix} = - \begin{bmatrix} \mathbf{R}_k^{\psi} \\ \mathbf{R}_k^{\omega} \end{bmatrix} \tag{32}$$

where

$$
\begin{aligned}
\left[\mathbf{K}_k^{\psi\psi}\right]_{i,j} &= \delta R_e \int_\Omega \phi_i^h \nabla\omega_k^h \cdot (\boldsymbol{B}\nabla\phi_j^h)\mathrm{d}\Omega \\
\left[\mathbf{K}_k^{\psi\omega}\right]_{i,j} &= \int_\Omega \nabla\varphi_i^h \cdot (\boldsymbol{A}\nabla\varphi_j^h)\mathrm{d}\Omega + \delta R_e \int_\Omega \varphi_i^h \nabla\varphi_j^h \cdot (\boldsymbol{B}\nabla\psi_k^h)\mathrm{d}\Omega \\
\left[\mathbf{K}_k^{\omega\psi}\right]_{i,j} &= \int_\Omega \nabla\varphi \cdot (\boldsymbol{A}\nabla\phi_j^h)\mathrm{d}\Omega \\
\left[\mathbf{K}_k^{\omega\omega}\right]_{i,j} &= \int_\Omega \varphi_i^h \varphi_j^h \mathrm{d}\Omega \\
\left[\mathbf{R}_k^{\psi}\right]_i &= \int_\Omega \nabla\phi \cdot (\boldsymbol{A}\nabla\omega_k^h)\mathrm{d}\Omega + \delta R_e \int_\Omega \phi \nabla\omega_k^h \cdot (\boldsymbol{B}\nabla\psi_k^h)\mathrm{d}\Omega \\
\left[\mathbf{R}_k^{\omega}\right]_i &= \int_\Omega \nabla\varphi \cdot (\boldsymbol{A}\nabla\psi_k^h)\mathrm{d}\Omega + \int_\Omega \varphi\psi_k^h \mathrm{d}\Omega,
\end{aligned}
\tag{33}
$$

and $\boldsymbol{\delta\psi}_k$ and $\boldsymbol{\delta\omega}_k$ are the vectors of nodal values of the k^{th} finite element update.

3.4 Evaluation of pressure

Piecewise continuous bi-quadratic isoparametric finite element shape functions are used to interpolate the unknown fields ψ and ω. However, derivatives of such shape functions are no longer continuous. Particularly, the derivatives are discontinuous across the element boundaries. Thus quantities that are derivatives of ψ and ω are evaluated only at the quadrature points in the interior of the elements. Gradient of the non-dimensional pressure field P can be calculated from partial derivatives of ψ and ω using the formula

$$
\nabla P = \boldsymbol{b} = \begin{bmatrix} R_e\delta\left(\dfrac{\partial\psi}{\partial x}\dfrac{\partial^2\psi}{\partial y^2} - \dfrac{\partial\psi}{\partial y}\dfrac{\partial^2\psi}{\partial x\partial y}\right) - \dfrac{\partial\omega}{\partial y} \\ \\ R_e\delta^3\left(\dfrac{\partial\psi}{\partial y}\dfrac{\partial^2\psi}{\partial x^2} + \dfrac{\partial\psi}{\partial x}\dfrac{\partial^2\psi}{\partial x\partial y}\right) - \delta^2\dfrac{\partial\omega}{\partial x} \end{bmatrix}
\tag{34}
$$

Instead of the usual way of evaluating pressure at the the quadrature points in the interior of the elements as a post-process, here we incorporated the weak form of pressure gradient equation (34) into (21). In which case, we are able to evaluate pressure at the nodal points and it is now piecewise continuous on Ω. The weak form of the pressure gradient equation (34) is given by

$$
\int_\Omega \nabla q \cdot \nabla P \mathrm{d}\Omega = \int_\Omega \nabla q \cdot \boldsymbol{b}\mathrm{d}\Omega,
\tag{35}
$$

where q is the pressure trial function. To find the pressure uniquely we need to have a Dirichlet boundary condition on either or both the inlet and outlet boundaries.

3.5 Mean pressure drop

Since the channel and the flow are symmetric the *mean pressure* $\bar{P}$ along any vertical line is equal to the pressure on the axis of the channel. That is

$$
\bar{P}(x) = P(x,0)
\tag{36}
$$

Furthermore, the mean pressure drop between $x = 0$ and $x = x_0$ is calculated using

$$
\Delta\bar{p}(x_0) \;=\; \bar{p}(0) - \bar{p}(x_0).
\tag{37}
$$

4 Results and discussion

The objective of this analysis is to study the behavior of an incompressible fluid flow through a channel of converging/diverging and slowly varying cross-section with absorbing walls by numerical approach. It may be recalled

that k characterize the slope of the converging/diverging wavy walls. $k = 1.0$ represents a diverging channel, $k = 0$ represents a normal (sinusoidal) channel and $k = -1.0$ represents a converging channel. ε and α represents amplitude and reabsorption coefficient of wavy walls. We discuss the effects of these parameters on the transverse velocity ($v(x,y)$), mean pressure drop ($\Delta\bar{p}(x)$) and stream function $\psi(x,y)$. In all our numerical calculations, the following parameters are fixed as $\delta = 0.1$ and $\varepsilon = 0.1$.

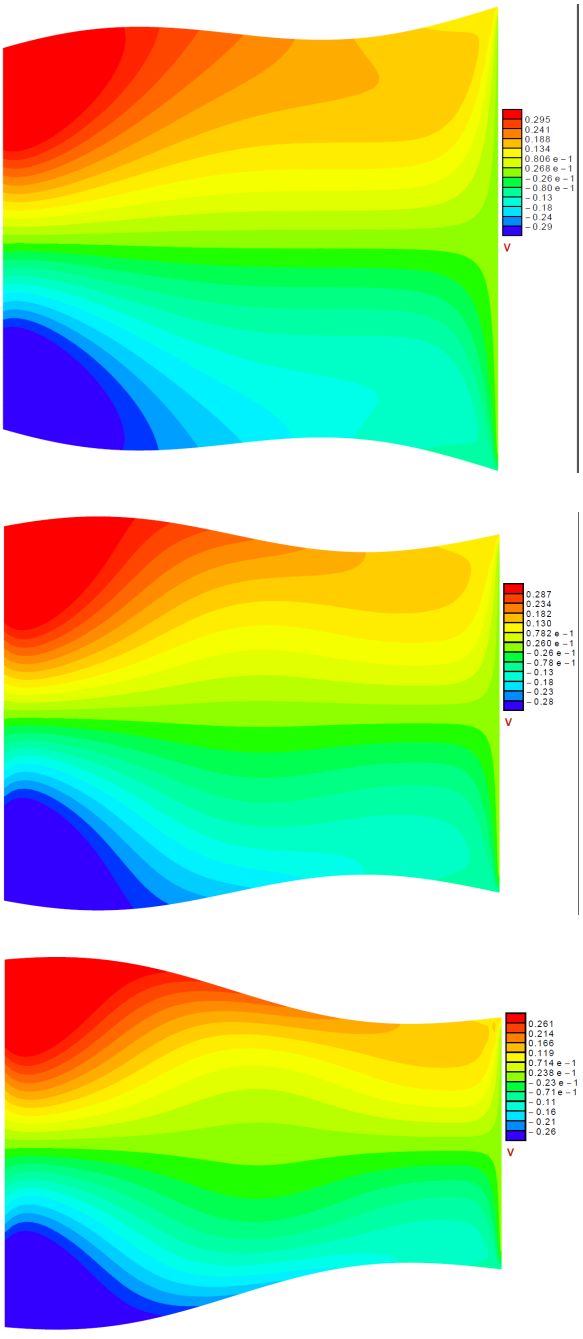

Fig. 3: A transverse velocity at k = 0.1, k = 0.0 and k = -0.1 respectively.

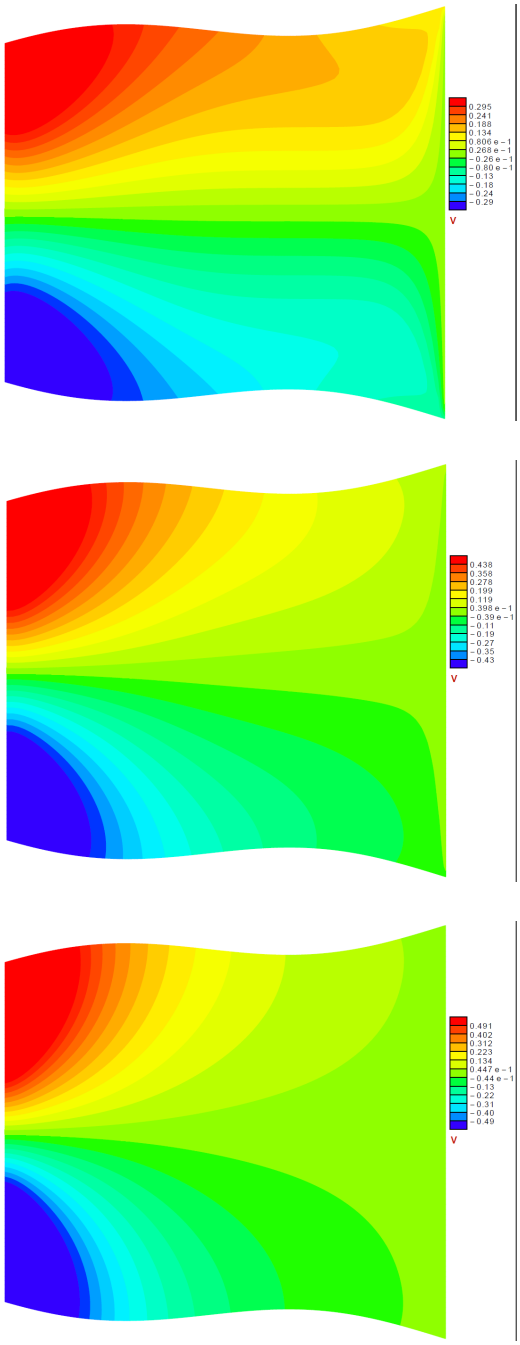

Fig. 4: A transverse velocity at α = 0.5, α = 1.0 and α = 1.5 respectively.

4.1 The velocity v

The velocity field can be obtained from approximation of the stream function. In this section, we discuss the effects of the slope parameter (k), reabsorption coefficient (α) and Reynolds number on the transverse velocity. Also, we look into the behavior of the velocity at different cross sections of the flow field. The effect of slope parameter (k) on the transverse velocity is shown in Figure (3). The velocity is more for divergent channel than the normal (sinusoidal) channel, and it is less for convergent channel than the other two. The effect of reabsorption coefficient α is presented in the Fig. (4). It can be observed from the figures that as α increases, the transverse velocity of the flow increases for all cases (converging, normal, and diverging channels).

Figure (5) illustrates the effect of Reynolds number on the velocity v versus y. As shown, the Reynolds number produces significant influence on the transverse velocity. As R_e increases from 0.1 to 100, the velocity increases and the point where the velocity attains its maximum decreases. Fig. 5 also shows the behavior of the velocity as the fluid passes through the channel at different locations of x. As the fluid passes from the entrance to exit, the transverse velocity decreases and it attains the maximum at the point $\cong 0.7$ at the entrance and it shifts towards the boundary at the exit.

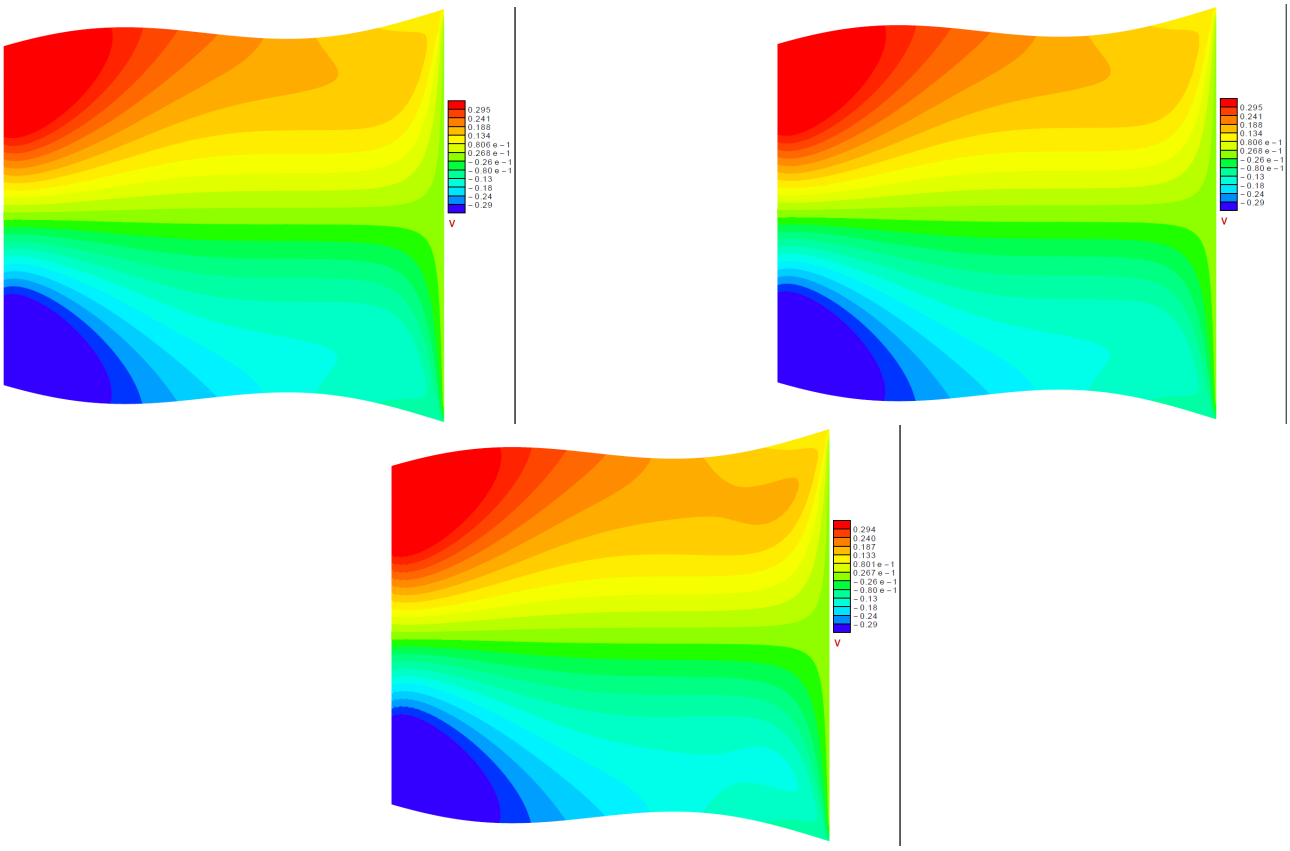

Fig. 5: A transverse velocity at R = 0.1, R = 50 and R = 100 respectively.

4.2 The velocity u

The reabsorption coefficient α and the slope parameter k has the same effect on the longitudinal velocity u. As α increases the velocity u decreases and it increases as the channel moves from diverging form to convergent form.

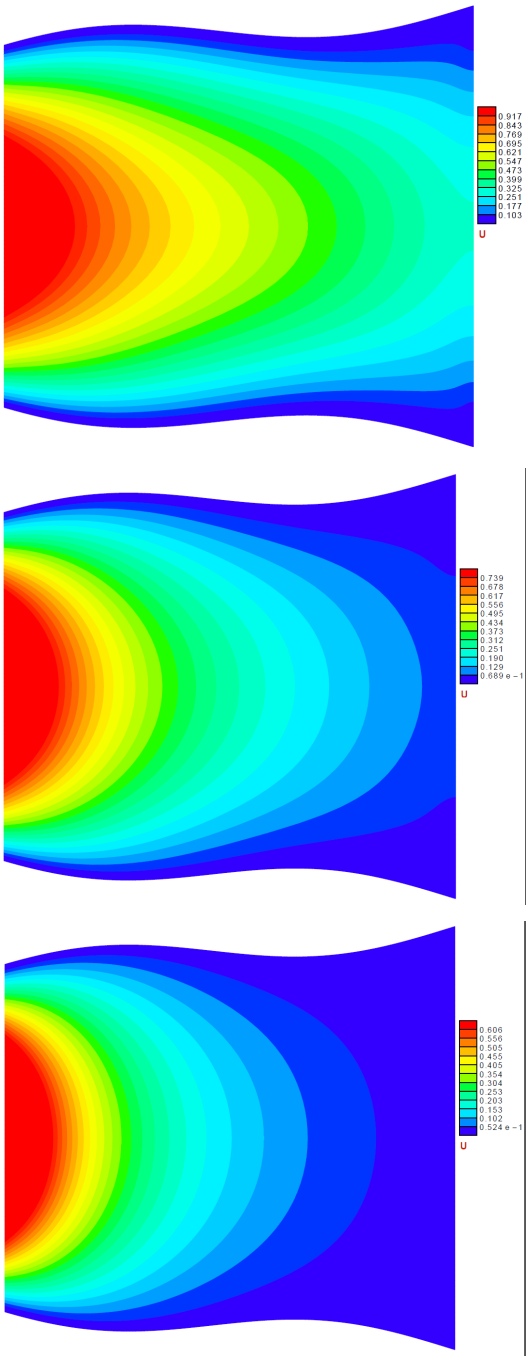

Fig. 6: A longitudinal velocity at α = 0.5, α = 1.0 and α = 1.5 respectively.

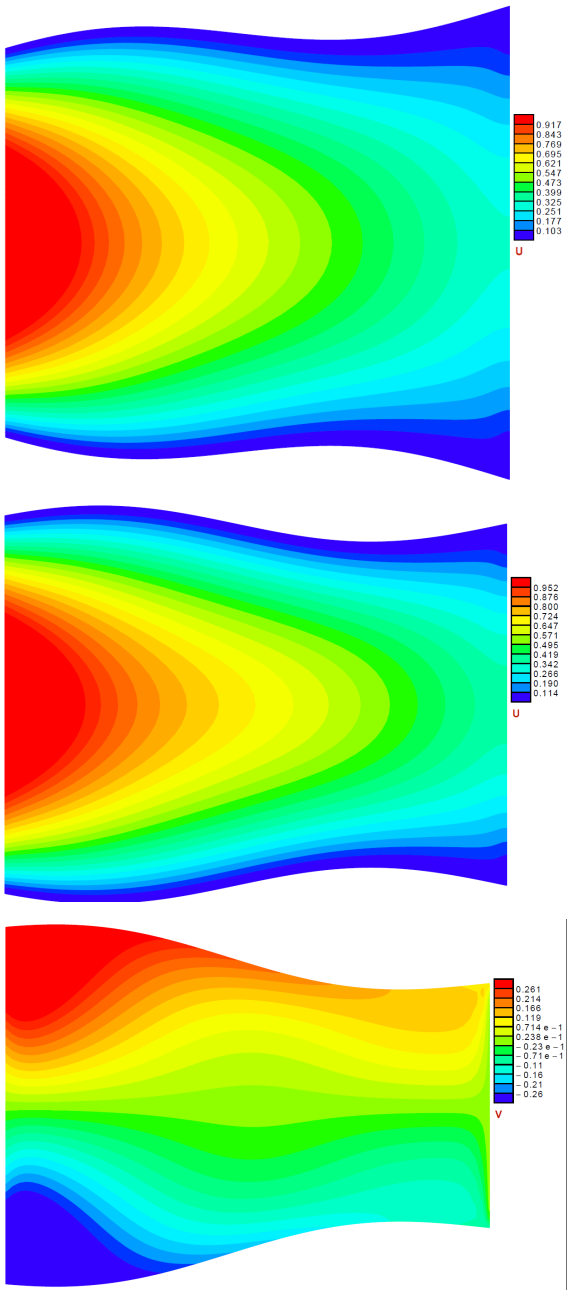

Fig. 7: A longitudinal velocity at k = 0.1, k = 0.0 and k = -0.1 respectively.

4.3 Pressure and mean pressure drop $\Delta \bar{p}$

The values of the mean pressure drop over the length of the channel are calculated for different values of k and α. As shown, in Figure 8, when the reabsorption coefficient α increases, the mean pressure drop decrease for all three forms of the channel (convergent, normal and divergent channels). Figure 9 displays the effect of slope parameter k to mean pressure drop. We can notice that $\Delta \bar{p}$ is less for the divergent channel than the normal or convergent channels, and it is more for convergent channel than the normal/divergent channels.

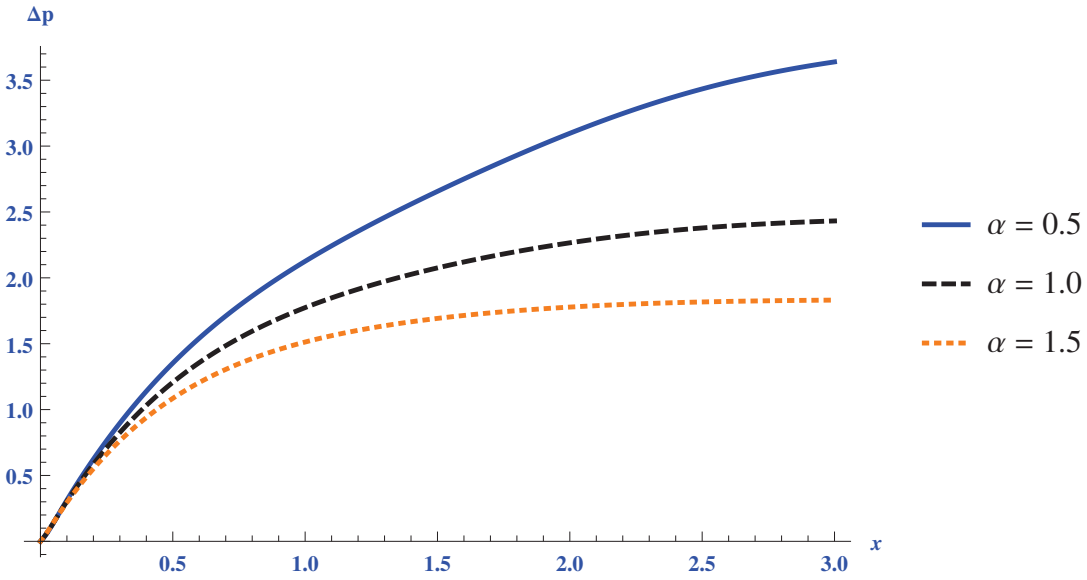

Fig. 8: Mean Pressure Drop at α = 0.5, α = 1.0 and α = 1.5 respectively.

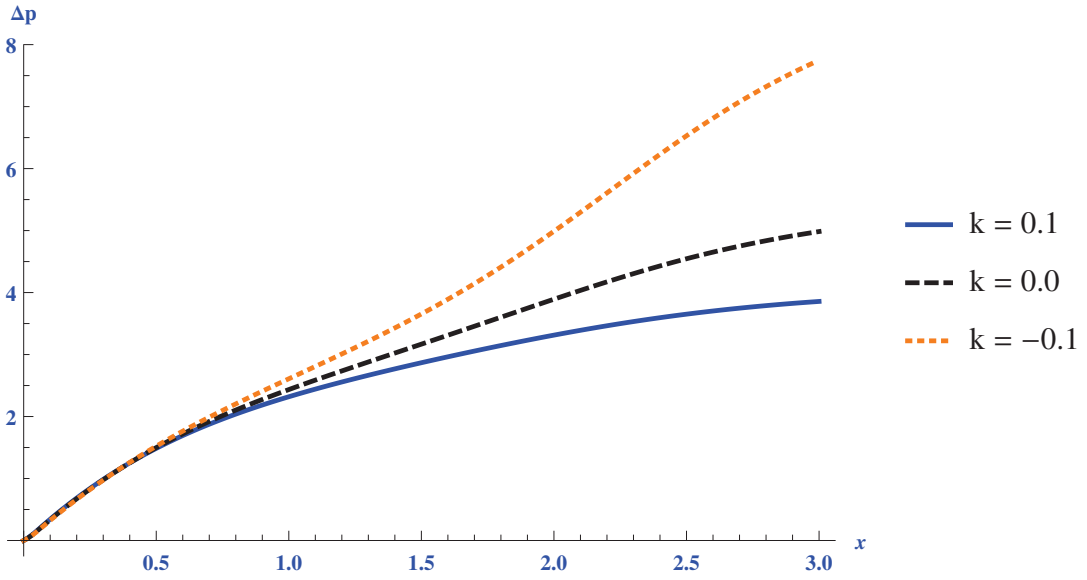

Fig. 9: Mean Pressure Drop at k = 0.1, k = 0.0 and k = -0.1 respectively.

Figures 10 - 13 shows the influence of α and k on the pressure p and mean pressure. These parameters has same effect on p and mean pressure. As the reabsorption coefficient α and slop parameter k increases the pressure decreases while the mean pressure rise.

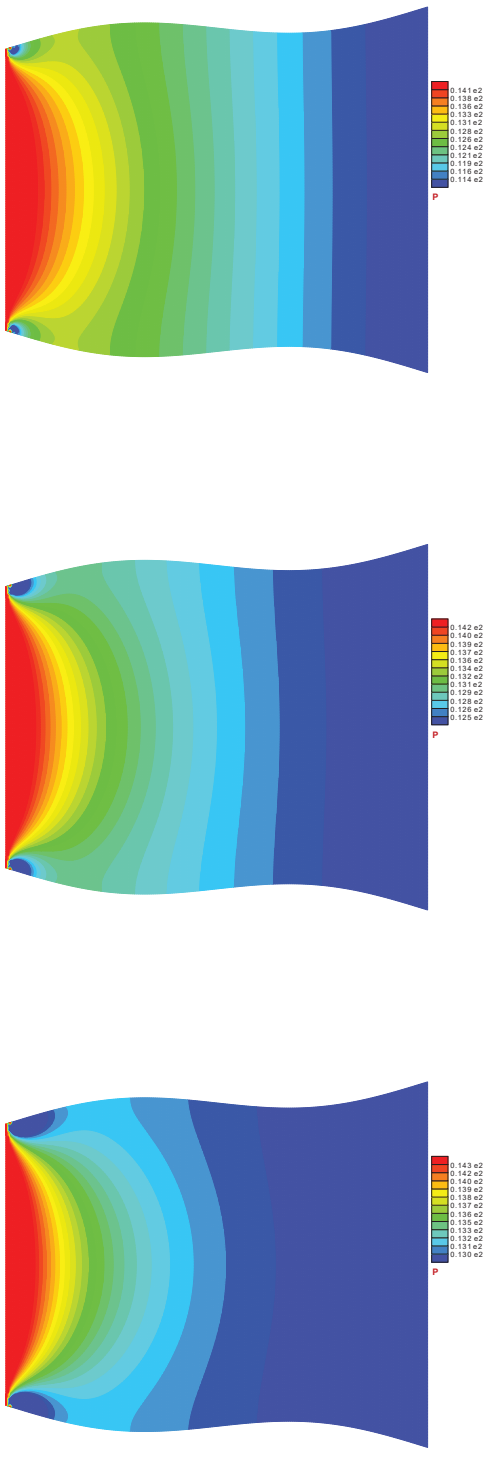

Fig. 10: Pressure at α = 0.5, α = 1.0 and α = 1.5 respectively.

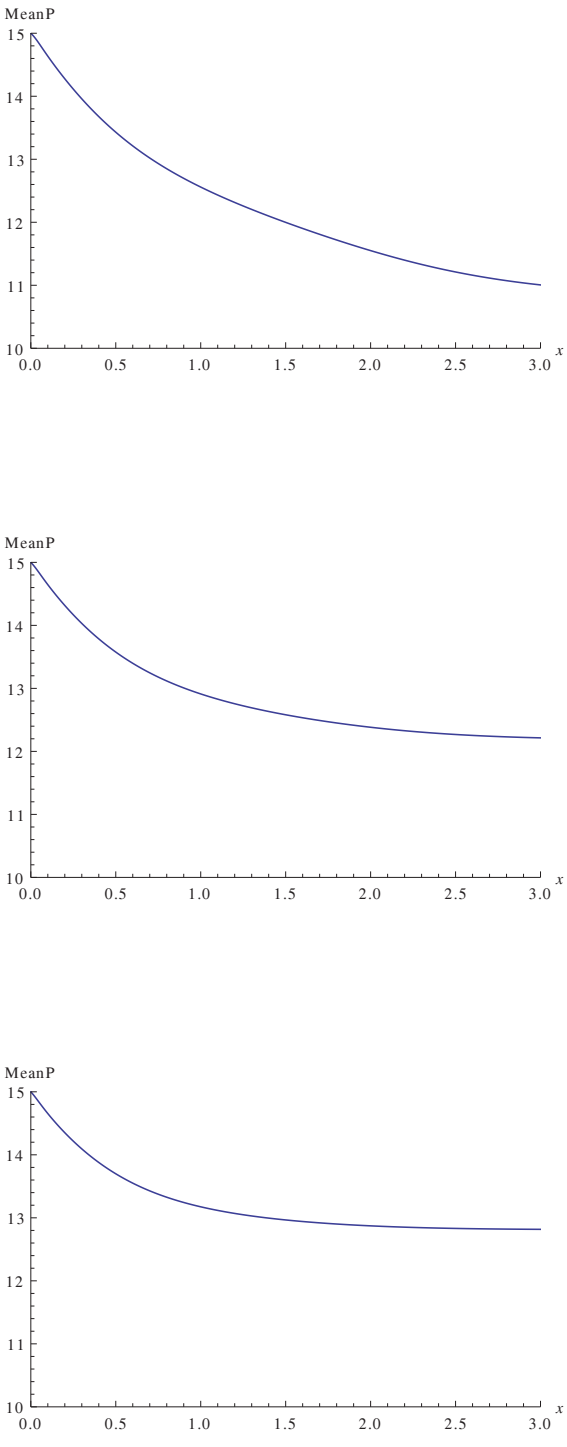

Fig. 11: Mean Pressure at α = 0.5, α = 1.0 and α = 1.5 respectively.

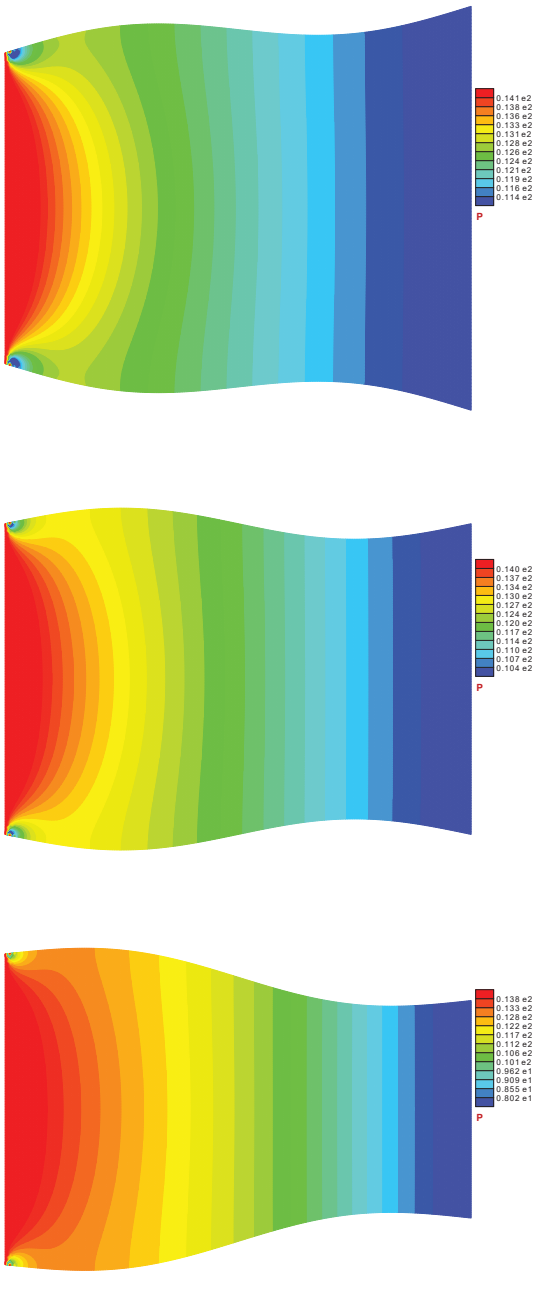

Fig. 12: Pressure at k = 0.1, k = 0.0 and k = -0.1 respectively.

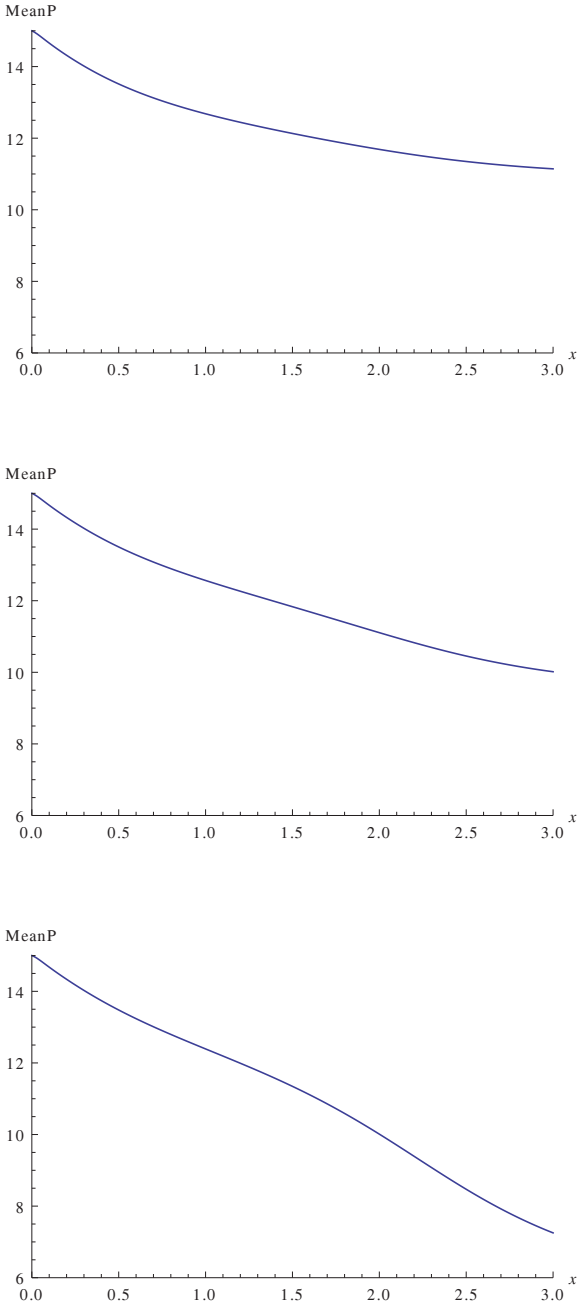

Fig. 13: Mean Pressure at $k = 0.1, k = 0.0$ and $k = -0.1$ respectively.

4.4 Stream function

We can observe the flow behavior of the fluid by looking at the contour drawing of the stream function for various values of reabsorption coefficient α and for the slope parameter k. Fig. (14) shows the effect of α on the flow behavior of the fluid. It can be observed that as α increases, the stream lines moves to the boundary because of more absorption. Fig. 15 are showing the flow pattern for diverging, normal(sinusoidal) and converging channels.

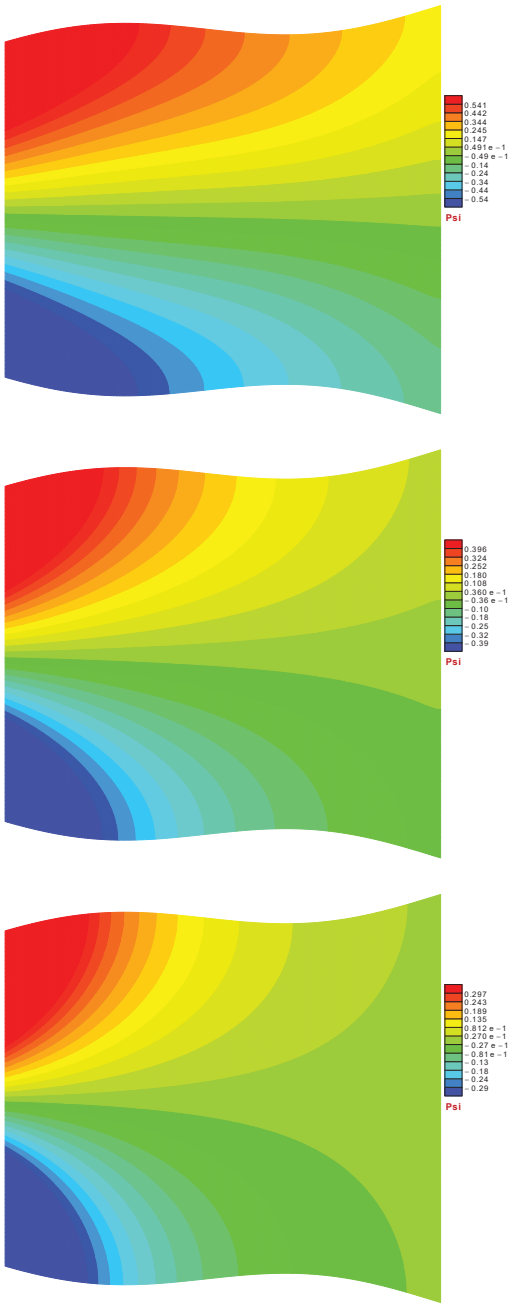

Fig. 14: Stream function at $\alpha = 0.5, \alpha = 1.0$ and $\alpha = 1.5$ respectively.

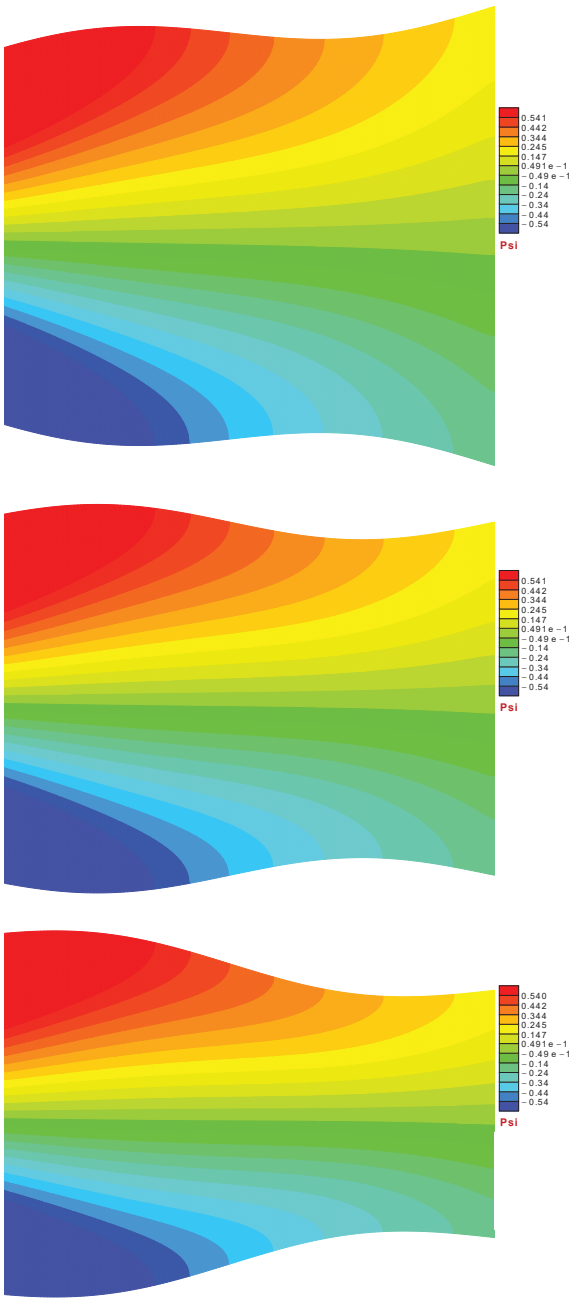

Fig. 15: Stream function at $k = 0.1, k = 0.0$ and $k = -0.1$ respectively.

5 Conclusions

In the present study, an analysis of mathematical model of incompressible fluid flow in a rigid channel of slowly varying converging/diverging walls has been presented with possible applications to the flow of fluid in renal tubules. The main contribution of this study is to use the numerical method to solve the Navier-Stock equations for an incompressible, steady, viscous flow without imposing any restriction on the parameters of the problem. The reabsorption coefficient α, the slope parameter k and the Reynolds number Re have the same effect on the transverse velocity. As they increases,

the velocity also increases. The mean pressure drop decreases for rise of reabsorption coefficient for all three forms of the channel (converging, normal(sinusoidal) and diverging channels). It is also less for the divergent channel than the normal or convergent channels, and it is more for convergent channel than the normal/divergent channels. The streamlines shows the general trend of the fluid flow. Physically, as the reabsorption coefficient increases the fluid that come out of the channel becomes very low.

Competing interests

The authors declare that they have no competing interests.

Authors' contributions

All authors have contributed to all parts of the article. All authors read and approved the final manuscript.

References

[1] R. I. Macey, Pressure flow patterns in a cylinder with reabsorbing walls, Bulletin of Mathematical Biophysics 25 (1963) 1–9.
[2] R. B. Kelman, A theoretical note on exponential flow in the proximal part of the mammalian nephron, Bulletin of Mathematical Biophysics 24 (1962) 303–317.
[3] R. I. Macey, Hydrodynamics in renal tubules, Bulletin of Mathematical Biophysics 27 (1965) 117–124.
[4] E. A. Marshall, E. A. Trowbridge, Flow of a newtonian fluid through a permeable tube: The application to the proximal renal tubule, Bulletin of Mathematical Biology 36 (1974) 457–476.
[5] P. J. Palatt, H. Sackin, R. I. Tanner, A hydrodynamical model of a permeable tubule, Journal of Theoretical Biology 44 (1974) 287–303.
[6] G. Radhakrisnamacharya, P. Chandra, M. R. Kaimal, A hydrodynamical study of the flow in renal tubules, Bulletin of Mathematical Biology 43 (2) (1981) 151–163.
[7] P. Chandra, J. S. V. R. K. Prasad, Low reynolds number flow in tubes of varying cross-section with absorbing walls, Jour. Math. Phy. Sci. 26 (1) (1992) 19–36.
[8] P. Chaturani, T. R. Ranganatha, Flow of newtonian fluid in non-uniform tubes with variable wall permeability with application to flow in renal tubules, Acta Mechanica 88 (1991) 11–26.
[9] P. Muthu, T. Berhane, Mathematical model of flow in renal tubules, International Journal of Applied Mathematics and Mechanics 6 (20) (2010) 94–107.
[10] P. Muthu, T. Berhane, Flow of newtonian fluid in non-uniform tubes with application to renal flow : A numerical study, Advances in Applied Mathematics and Mechanics 3 (5) (2011) 633–648.
[11] E. F. Elshehawey, E. M. Elbarbary, N. S. Elgazery, Effect of inclined magnetic field on magneto fluid flow through a porous medium between two inclined wavy porous plates (numerical study), Applied Mathematics and Computation 135 (2003) 85–103.
[12] B. V. R. Kumar, K. B. Naidu, A numerical study of peristaltic flows, Computers & fluids 24 (2) (1995) 161–176.
[13] T. J. Hughes, The finite element method: linear static and dynamic finite element analysis, Courier Corporation, 2012.
[14] A. G. Holzapfel, Nonlinear solid mechanics, Vol. 24, Chichester: Wiley, 2000.